Full Length Article

Zoledronate and Raloxifene combination therapy enhances material and mechanical properties of diseased mouse bone

Katherine M. Powell[a], Cayla Skaggs[a], Alexis Pulliam[a], Alycia Berman[b], Matthew R. Allen[c], Joseph M. Wallace[a,*]

[a] *Department of Biomedical Engineering, Indiana University-Purdue University at Indianapolis, Indianapolis, IN, USA*
[b] *Weldon School of Biomedical Engineering, Purdue University, West Lafayette, IN, USA*
[c] *Department of Anatomy and Cell Biology, Indiana University School of Medicine, Indianapolis, IN, USA*

ARTICLE INFO

ABSTRACT

Current interventions to reduce skeletal fragility are insufficient at enhancing both the quantity and quality of bone when attempting to improve overall mechanical integrity. Bisphosphonates, such as Zoledronate (ZOL), are used to treat a variety of bone disorders by increasing bone mass to decrease fracture risk, but long-term use has been shown in some settings to compromise bone quality. Alternatively, Raloxifene (RAL) has recently been demonstrated to improve tissue quality and overall mechanical properties in a cell-independent manner by binding to collagen and increasing tissue hydration. We hypothesized that a combination of RAL and ZOL would improve mechanical and material properties of bone more than either monotherapy alone by enhancing both quantity and quality. In this study, wildtype (WT) and heterozygous (OIM + / −) male mice from the Osteogenesis Imperfecta (OI) murine model were treated with either RAL, ZOL, or both from 8 weeks to 16 weeks of age. Using the OIM model allows for investigation of therapeutic effects on a quality-based bone disease. Combination treatment resulted in higher trabecular architecture, cortical mechanical properties, and cortical fracture toughness in diseased mouse bone. Two fracture toughness properties, which are direct measures of the tissue's ability to resist the initiation and propagation of a crack, were significantly improved with combination treatment in OIM + / − compared to control. There was no significant effect on fracture toughness with either monotherapy alone in either genotype. Following the mass-based effects of ZOL, trabecular bone volume fraction was significantly higher with combination treatment in both genotypes. Combination treatment resulted in higher ultimate stress in both genotypes. RAL and combination treatment in OIM + / − also increased resilience compared to the control. In conclusion, this study demonstrates the beneficial effects of using combination drug treatments to increase bone mass while simultaneously improving tissue quality, especially to enhance the mechanical integrity of diseased bone. Combination therapies could be a potential method to improve bone health and combat skeletal fragility on both the microscopic and macroscopic levels.

1. Introduction

Bisphosphonates (BPs) have been the gold standard to treat skeletal fragility and numerous bone disorders for the past 30 years. BPs increase bone mineral density which leads to decreased fracture risk in diseases such as postmenopausal osteoporosis, Paget's disease, metastatic osteolytic lesions, and more recently, Osteogenesis Imperfecta (OI) [1–3]. BPs target osteoclasts and decrease their activity, which ultimately leads to the disruption of the bone remodeling process [4]. However, long term BP use may have unintended consequences. The disruption of bone remodeling reduces the bone repair mechanism which can lead to the accrual of microdamage in the tissue, making the tissue more susceptible to failure [5]. BP use has also demonstrated an increase of non-enzymatic cross linking in the collagen matrix, which has been correlated with reduced post-yield mechanical properties [6–8]. Despite the positive mass-based effects BPs have in bone, tissue quality may not be optimal, making these treatments insufficient to overcome mechanical deficits that commonly manifest with disease. There is a need to simultaneously improve tissue quality while increasing mass.

Raloxifene (RAL) is in a different class of FDA-approved drugs used to treat osteoporosis in post-menopausal women. The drug primarily
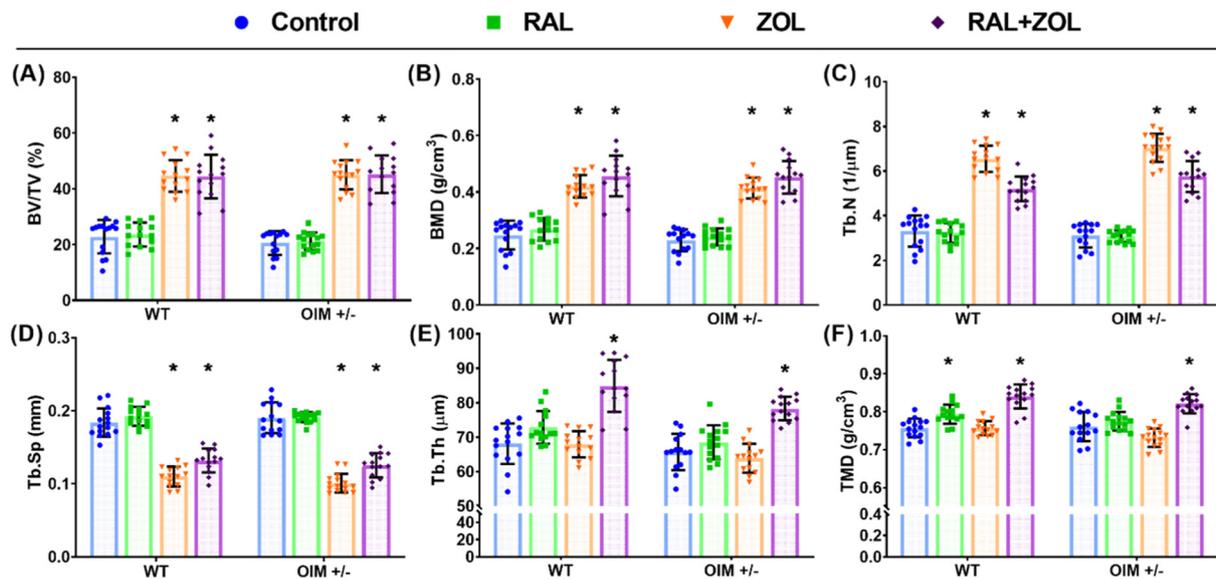

Fig. 1. Treatment effects on (A) bone volume fraction (BV/TV), (B) bone mineral density (BMD), (C) trabecular number (Tb.N), (D) trabecular separation (Tb.Sp), (E) trabecular thickness (Tb.Th), and (F) tissue mineral density (TMD) in the distal femoral metaphysis. Significant change from control indicated by '*' at $p < 0.05$.

acts in a cell-dependent manner as a Selective Estrogen Receptor Modulator (SERM) and combats bone loss by binding and signaling through estrogen receptors on osteoblasts [9]. Clinically, RAL reduces fractures by ~50% but with modest changes in remodeling and bone mineral density (BMD) [10–12]. This observation suggests that the changes in mechanical integrity are driven by tissue quality changes versus altered mass or architecture. Recent work has demonstrated that RAL also exhibits cell-independent behavior by binding to collagen and increasing tissue hydration, leading to enhanced mechanical properties and fracture resistance [13,14]. These cell-independent, material-based changes provide a unique opportunity to beneficially alter bone fracture resistance through changes in tissue quality, especially in disease states that are driven by inferior tissue properties.

OI is a genetic disease in bone caused by a mutation in Type I collagen or related proteins. The mutated collagen leads to poor formation of the triple helical structure, driving quality-based deficiencies in the collagen-mineral composite [15–17]. These microscopic changes induce macroscopic effects and cause brittle bones and frequent fractures in patients suffering from the disease. The majority of fractures in OI patients occur at cortical regions of their long bones, and the femoral mid-diaphysis is particularly at risk due to load bearing during ambulation [18,19]. Targeting quality at these regions is crucial to clinically reduce fractures in patients affected by OI.

Previously, clinical research has shown potential benefits of using the combination of RAL and ZOL in osteoporotic women [20]. However, combination treatment has not been assessed in a disease where the mechanical deficits root from microscopic-level deficiencies in quality. In this study, the osteogenesis imperfecta murine (oim) model of OI allowed for investigation of how combination treatments impact the phenotype of a quality-based disease state [21], where adding more, poor quality, tissue with BPs might not be enough to overcome mechanical deficiencies. It was hypothesized that using the mass-based effects of BPs, in conjunction with the tissue level improvements noted with RAL, would improve bone mechanical properties and fracture resistance more than either monotherapy alone.

2. Materials and methods

2.1. Animals and treatment

All protocols and procedures were performed with prior approval

from the IU School of Medicine IACUC. Male wild-type (WT) and heterozygous (OIM $+/-$) mice were bred from heterozygous parental strains on a C57BL/6 background [22]. Beginning at 8 weeks of age, mice ($n = 13–15$ per group) were injected subcutaneously with either RAL (0.5 mg/kg; 5×/week), zoledronate (ZOL; 80 μg/kg; at 8 weeks and 12 weeks of age), or the combination. Untreated controls were also included. These dosages were chosen based on previous research showing efficacy in vivo [23–26]. At 16 weeks of age, the mice were euthanized by CO_2 asphyxiation, and the right femora and tibiae were harvested, stripped of soft tissue, and frozen wrapped in phosphate buffered saline (PBS)-soaked gauze at $-20\,°C$.

2.2. Microcomputed tomography (μCT) and architectural analysis

To determine the effects of treatment on bone architecture, right femora were scanned using a nominal voxel size of 10 μm (Skyscan 1172, Bruker). Scans were performed using a 0.7-degree angle increment, two frames averaged, through a 0.5 mm Al filter (V = 60 kV, $I = 167$ μA). Images were reconstructed (nRecon) and calibrated to hydroxyapatite-mimicking phantoms (0.25 and 0.75 g/cm³ Ca-HA). For each femur, a cancellous region was selected at the distal metaphysis, extending 1-mm proximally from the most proximal portion of the growth plate, and then quantified using CT Analyzer (CTAn). To obtain cortical architectural properties, a 1-mm cortical region was selected at approximately 50% length of the femur, then analyzed with a custom MATLAB script [27]. Additionally, right tibiae were scanned at the mid-diaphysis to obtain cortical geometry used for fracture toughness testing as indicated below.

2.3. Three-point bending mechanical testing to failure

Right femora were tested to failure in three-point bending (support span at 8 mm) with the anterior surface in tension. The bones were loaded at a displacement control rate of 0.25 mm/s while the sample remained hydrated with PBS. Cross-sectional cortical properties at the femoral mid-diaphysis were obtained from μCT images as described above. These properties were used to map load-displacement data into stress-strain data using standard engineering equations as previously reported [28].

Table 1
Cortical geometry at the femoral mid-diaphysis.

	WT					OIM+/−				
	Control	RAL	ZOL	RAL + ZOL	p-Value	Control	RAL	ZOL	RAL + ZOL	p-Value
Total CSA (mm²)	2.031 ± 0.174	2.068 ± 0.193	2.011 ± 0.216	2.053 ± 0.19	0.877	1.897 ± 0.267	1.837 ± 0.167	1.965 ± 0.31	1.834 ± 0.194	0.712
Marrow Area (mm²)	1.051 ± 0.1	1.047 ± 0.116	1.027 ± 0.104	1.028 ± 0.102	0.891	0.974 ± 0.128	0.902 ± 0.096	0.979 ± 0.157	0.906 ± 0.116	0.273
Cortical Area (mm²)	0.98 ± 0.113	1.02 ± 0.084	0.984 ± 0.129	1.024 ± 0.107	0.583	0.923 ± 0.179	0.935 ± 0.092	0.987 ± 0.176	0.929 ± 0.091	0.951
Cortical Thickness (mm)	0.227 ± 0.021	0.235 ± 0.01	0.23 ± 0.021	0.238 ± 0.017	0.371	0.225 ± 0.04	0.231 ± 0.017	0.238 ± 0.036	0.229 ± 0.013	0.939
Periosteal perimeter (mm)	5.868 ± 0.231	5.921 ± 0.239	5.852 ± 0.271	5.898 ± 0.24	0.881	5.684 ± 0.357	5.63 ± 0.25	5.789 ± 0.395	5.611 ± 0.254	0.758
Endocortical perimeter (mm)	4.581 ± 0.224	4.533 ± 0.242	4.53 ± 0.282	4.5 ± 0.218	0.839	4.414 ± 0.301	4.286 ± 0.265	4.513 ± 0.543	4.247 ± 0.256	0.327
I_{max} (mm⁴)	0.346 ± 0.064	0.366 ± 0.061	0.347 ± 0.074	0.366 ± 0.067	0.739	0.3 ± 0.084	0.301 ± 0.058	0.329 ± 0.081	0.292 ± 0.058	0.839
I_{min} (mm⁴)	0.168 ± 0.031	0.177 ± 0.035	0.165 ± 0.041	0.174 ± 0.035	0.826	0.151 ± 0.045	0.139 ± 0.025	0.166 ± 0.073	0.142 ± 0.032	0.738
TMD (g/cm³)	1.272 ± 0.021	1.267 ± 0.048	1.277 ± 0.024	1.28 ± 0.021	0.698	1.309 ± 0.032	1.314 ± 0.031	1.307 ± 0.035	1.314 ± 0.037	0.954

Values are presented as mean ± standard deviation. CSA - cross sectional area; I_{max} - maximum moment of inertia; I_{min} - minimum moment of inertia; TMD - tissue mineral density. There was not a main ANOVA effect in any of the properties.

2.4. Fracture toughness testing

Fracture toughness of the right tibiae was measured using a linear elastic fracture mechanics approach, as described previously [29,30]. Briefly, a notch was made on the anteromedial aspect of the tibia, at approximately 50% of the length, using a scalpel blade lubricated with a 1 μm diamond suspension. The tibiae were notched into the medullary cavity to a depth not exceeding the bone's midpoint. They were then tested to failure in 3-point bending at a displacement control rate of 0.001 mm/s with the notched surface in tension. The load point was positioned directly above the notch site.

After mechanical testing, the bones were cleansed of marrow and dehydrated using an ethanol gradient (70–100%) and a vacuum desiccator. Following sputter-coating with gold, the cross-sectional fracture surface was imaged with scanning electron microscopy (SEM). The angles of stable and unstable crack growth were obtained from the images and, along with geometric properties from μCT data, a custom MATLAB script calculated stress intensity factors for crack initiation, maximum load, and fracture instability.

2.5. Statistical analysis

All data were checked for assumptions of normality and homogeneity of variance, and violations were corrected using transformations. For each genotype independently, a One-Way ANOVA with posthoc Dunnett's test was used to statistically analyze the effect of each treatment versus control. Analysis was performed using GraphPad Prism (v.8) with a significance level at α = 0.05.

3. Results

3.1. Treatment contributed to gains in trabecular architecture and mineralization

Bone volume fraction and bone mineral density in the femoral distal metaphysis were significantly greater compared to control in both genotypes with ZOL monotherapy and combination treatment, but not with RAL monotherapy (Fig. 1, Supplemental Tables 1 and 3). Similarly, in both genotypes, trabecular number was significantly greater and trabecular spacing significantly lower with ZOL alone and with combinatorial therapy but not with RAL alone. Although trabecular thickness trended upward with RAL in both WT (+7.1%) and OIM +/− (+5.8%), it only reached significance with combination treatment in both genotypes (WT: +24.7%; OIM+/−: +20.9%). Tissue mineral density (TMD) was significantly elevated with the combination treatment in both genotypes. Additionally, TMD significantly increased in WT mice with RAL monotherapy. Although the property trended upward in OIM+/− with RAL alone, it did not reach significance. ZOL had no effect on TMD in either genotype.

3.2. Treatment had no effect on cortical geometry at the femoral mid-diaphysis

Despite the large changes in cancellous bone architecture, cortical geometric properties showed no significant changes with either monotherapy or combinatorial treatment at the femoral mid-diaphysis (Table 1).

3.3. Treatments increased femoral mechanical strength and stiffness

The majority of significant effects noted in femoral mechanical properties occurred in strength parameters (Fig. 2, Tables 2 and 3, and Supplemental Table 3). At the structural level, RAL monotherapy and combination treatment resulted in higher yield force in both genotypes. ZOL monotherapy also significantly increased the property but only in WT. Ultimate force was significantly elevated compared to control with
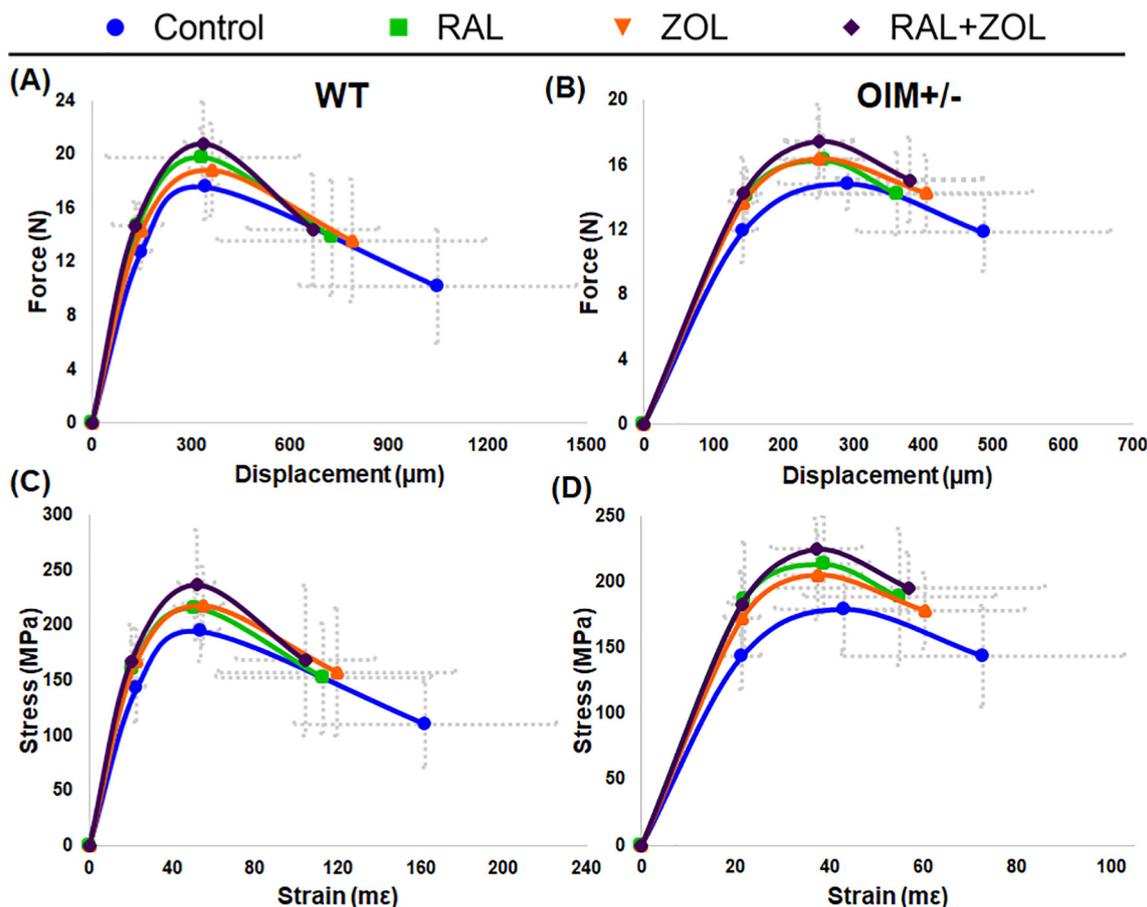
Fig. 2. Schematic force-displacement curves for WT (A) and OIM +/− (B). Schematic stress-strain curves for WT (C) and OIM +/− (D).

combination treatment in both genotypes. In WT, total displacement was significantly lower with RAL and combination treatment compared to control.

At the tissue level, ultimate stress was significantly higher with combination treatment compared to control in both genotypes. RAL alone increased ultimate stress in OIM+/− but not in WT. Yield stress significantly increased with all treatments in OIM+/−. Although the property trended up in WT, it did not reach significance ($p = 0.10$). Higher yield stress led to greater resilience in OIM+/− with RAL and combination treatment versus control, but not with ZOL alone. Following the displacement trend, total strain in WT was significantly lower with combination treatment.

A few non-strength parameters were also impacted by treatment. Stiffness was significantly higher with all treatments in OIM +/−, but in WT, only increased with RAL monotherapy and combination therapy. The combination treatment in WT also resulted in a greater modulus and decreased total strain compared to control.

3.4. Fracture toughness was elevated in OIM+/− with combination treatment

Combination treatment in OIM+/− led to significantly higher stress intensity factors at crack initiation and maximum load at the tibial mid-diaphysis (Fig. 3, Supplemental Tables 2 and 3). Neither monotherapy significantly changed fracture toughness in OIM+/−. Treatment in WT produced no significant effects in the stress intensity factors.

4. Discussion

Current therapeutics used to combat bone fragility are able to

increase bone mass but are insufficient on their own to enhance bone quality and improve fracture resistance in some diseased states. Targeting different mechanisms with a combination treatment could be a powerful technique to enhance bone on both a macroscopic (mass) and microscopic tissue (quality) level. The goal of this study was to investigate how the mass-based effects of bisphosphonates, combined with the tissue-level improvements seen with Raloxifene, would improve bone quantity, quality, and fracture resistance. The results demonstrate that ZOL and RAL could be used together to enhance trabecular architecture, cortical mechanical properties, and tissue fracture toughness more than either treatment alone, a finding that was more pronounced in diseased bone.

For trabecular architecture, the combination treatment appeared to be driven by the dominant effects of ZOL, with greater bone volume fraction, greater trabecular number, and lower trabecular spacing. ZOL alone did not impact trabecular thickness or TMD. These trabecular findings are consistent with previous research investigating BP use in adolescent OI mice [31–34]. The results are unsurprising as at this relatively young age, trabecular bone is often lost with longitudinal growth coupled with resorptive modeling in mice. BP use effectively inhibited this modeling and bone volume was maintained.

Although RAL exhibited an overall minimal effect on trabecular structure, there was a trend toward increased trabecular thickness and TMD. Similar changes to thickness and TMD have previously been noted with RAL use [26,32]. The properties did not change with ZOL alone, but with combination therapy, the improvements were synergistic in both genotypes, producing greater than three times the effect of either monotherapy in most cases. Increased thickness with RAL was likely initiated by the cellular anabolic effects of RAL as a SERM drug. When adding ZOL, the resorptive modeling that would have otherwise occurred at the struts was inhibited, and thickness was

Table 2
Structural mechanical properties from 3-point bending of the femoral mid-diaphysis.

| | WT | | | | | OIM+/− | | | | |
	Control	RAL	ZOL	RAL + ZOL	p-Value	Control	RAL	ZOL	RAL + ZOL	p-Value
Yield force (N)*#	12.7 ± 1.3	14.7 ± 1.6**	14.3 ± 2*	14.7 ± 1.8**	0.007	11.9 ± 2	14.1 ± 1.7**	13.7 ± 1.8	14.3 ± 2.2**	0.008
Ultimate force (N)*#	17.6 ± 2.4	19.8 ± 2.1	18.8 ± 3.4	20.8 ± 3.1**	0.023	14.8 ± 1.6	16.2 ± 1.6	16.4 ± 2.5	17.4 ± 2.2**	0.011
Displ. to yield (μm)	148.4 ± 30.6	138.5 ± 21.9	148.8 ± 17.3	130.6 ± 12.8	0.092	142.9 ± 18.9	147 ± 12.8	142.1 ± 20.4	142.8 ± 16.1	0.862
Post yield Displ. (μm)*	899.9 ± 417	590.8 ± 291.5	638.9 ± 395.6	539.6 ± 196*	0.029	343.8 ± 177.3	215.7 ± 120.3	261.7 ± 156.5	238.2 ± 100.6	0.096
Total displ. (μm)*	1048.3 ± 421.5	729.3 ± 292.5*	787.8 ± 407.1	670.2 ± 197.6*	0.024	486.6 ± 181.4	362.7 ± 121.6	403.9 ± 152	381 ± 104.3	0.111
Stiffness (N/mm)*#	97.7 ± 18.9	120.1 ± 19.7**	107.9 ± 21.7	125.8 ± 14.5***	< 0.001	92.4 ± 9.9	107 ± 14.5*	107.9 ± 17*	111.5 ± 16**	0.006
Work to yield (mJ)	1.02 ± 0.23	1.11 ± 0.23	1.15 ± 0.17	1.05 ± 0.2	0.386	0.93 ± 0.25	1.13 ± 0.19	1.06 ± 0.25	1.12 ± 0.24	0.103
Post yield work (mJ)	11.2 ± 4.29	9.46 ± 4.33	9.36 ± 4.27	9.62 ± 3.52	0.587	4.61 ± 2.49	3.1 ± 1.51	3.97 ± 2.48	3.79 ± 1.69	0.289
Total work (mJ)	12.22 ± 4.22	10.57 ± 4.37	10.51 ± 4.37	10.67 ± 3.6	0.633	5.54 ± 2.55	4.23 ± 1.47	5.03 ± 2.5	4.9 ± 1.82	0.431

Values are presented as mean ± standard deviation. In the property column, a significant main effect of treatment is indicated by '*' in WT and '#' in OIM+/− . A significant difference from control within each genotype is indicated by '*' for $p < 0.05$, '**' for $p < 0.01$, and '***' for $p < 0.001$. Displ. – displacement.

maintained and elevated compared to control. It is unclear why TMD was amplified with combination treatment, but this positive effect deserves additional investigation.

Although trabecular architecture was enhanced and this positive effect cannot be overlooked, clinical fractures typically occur at cortical locations in the diaphysis rather than the metaphyses, and improved trabecular features does not necessarily address the problem of fracture resistance. In this current study, there were no significant effects on cortical geometry with any treatment in either genotype. Previous work has shown that, in cortical bone, metabolic activity is lower, and it was expected that ZOL would have little effect on mass [31–34]. Likewise, RAL is expected to have limited geometric effect in cortical locations. However, previous work has demonstrated significant increases in cortical thickness that were not reproduced in this study [26,32]. This discrepancy could be due to differences in animal age, as one of the studies investigated mice at from 16 weeks to 24 weeks, or phenotype severity, as the other study used homozygous OI mice bred on a mixed B6/C3H background.

Regardless, the lack of geometric changes suggests that any differences in mechanical properties are most likely driven by changes at the intrinsic tissue level. Greater intracortical porosity has been demonstrated in pediatric OI bone, which negatively impacts cortical mechanical integrity [35,36], but intracortical porosity was not observed here. Given that the majority of clinical fractures occur at cortical regions in OI pediatric patients, further insight on pharmacological improvements of cortical bone porosity and quality should be investigated.

The significant effects of treatment versus control on mechanical behavior were mostly related to strength parameters. The tissues had increased stiffness with all the treatments. ZOL had a modest impact on its own, significantly increasing yield force in WT and yield stress in OIM+/− . The effects of RAL alone were more compelling and drove the changes seen with combination treatment. Yield stress increased in OIM+/− with RAL and combination treatment which led to a significant increase in resilience, indicating the bones were able to absorb more energy before yielding.

Previous work with RAL has demonstrated enhanced post-yield mechanical behavior with bone soaked ex-vivo, one year of treatment in female beagles, and with RAL administration after first treating with ZOL in mice [13,23,32]. In this study, treatment groups did not show increased post-yield properties and, in some cases, surprisingly decreased. This is common with BP use, but a significant decrease in post-yield behavior with RAL was unexpected. Previous work with OI mice at this age range demonstrated no significant effect of in-vivo RAL treatment on any whole bone mechanical properties [26]. In the current study, control groups from both genotypes showed far more total deformation than expected, causing treatment effects to appear significantly lower compared to control. The reason behind these effects is not clear, but it removed the possibility of detecting any potential post-yield effects of treatment.

Perhaps the most important result here is that the combination treatment improved stress intensity factors at crack initiation and maximum load in the diseased mice. This type of test reflects true material-level properties in bone and indicates improved fracture resistance in diseased bone with this combined treatment. It was hypothesized that increasing mass at the same time as improving quality would benefit fracture resistance more than either monotherapy alone. The argument for this is that when more bone is formed in the presence of a compound that enhances quality, the combined tissue-level impact should be large. Because ZOL did not improve cortical mass as expected, and RAL alone did not improve fracture toughness, the improvement with combined treatment is curious. The mechanism behind this change is not known, but future investigation of tissue quality changes should help to clarify. Treatment did not impact WT mice, likely because it is difficult to improve bone that is already of good quality. Similar to the results of this study, fracture toughness has not

Table 3
Estimated tissue-level mechanical properties from 3-point bending of the femoral mid-diaphysis.

	WT					OIM +/−				
	Control	RAL	ZOL	RAL + ZOL	p-Value	Control	RAL	ZOL	RAL + ZOL	p-Value
Yield stress (MPa)[#]	143 ± 30.8	161 ± 24.3	167.2 ± 29.5	167.3 ± 33.7	0.104	143.3 ± 24.4	187 ± 42.5**	172.5 ± 35.6*	183.2 ± 17.4**	0.002
Ultimate stress (MPa)*#	194.3 ± 26.7	215.5 ± 20.3	217.7 ± 35.5	236.6 ± 49.3**	0.020	179.3 ± 30.5	213.3 ± 37.1*	205.4 ± 34	224.7 ± 23.3**	0.003
Strain to yield (mε)	22.9 ± 3.9	21.0 ± 3.5	22.7 ± 2.8	20.1 ± 1.9	0.060	21.3 ± 4.1	21.9 ± 2.3	21.4 ± 3.8	21.3 ± 3.3	0.949
Total strain (mε) *	162.3 ± 63.5	113.2 ± 52	119.6 ± 57.2	104.3 ± 33.4*	0.023	72.9 ± 30.1	55 ± 20.5	60.2 ± 21.4	57 ± 16.8	0.162
Modulus (GPa)*	6.92 ± 1.19	8.65 ± 1.6	8.33 ± 2.54	9.39 ± 2.34**	0.013	7.74 ± 2.19	9.69 ± 3.2	9.09 ± 2.11	9.76 ± 1.82	0.106
Resilience (MPa)[#]	1.8 ± 0.62	1.85 ± 0.49	2.03 ± 0.35	1.83 ± 0.39	0.567	1.64 ± 0.38	2.2 ± 0.43**	2.03 ± 0.69	2.13 ± 0.4*	0.017
Toughness (MPa)	21.3 ± 7.6	17.34 ± 6.27	18.53 ± 7.63	18.28 ± 5.71	0.456	9.66 ± 4.03	8.12 ± 2.68	9.15 ± 3.84	9.23 ± 2.78	0.650

Values are presented as mean ± standard deviation. In the property column, a significant main One-Way ANOVA effect of treatment is indicated by '*' in WT and '#' in OIM +/−. A significant difference from control within each genotype is indicated by '*' for $p < 0.05$, '**' for $p < 0.01$, and '***' for $p < 0.001$.
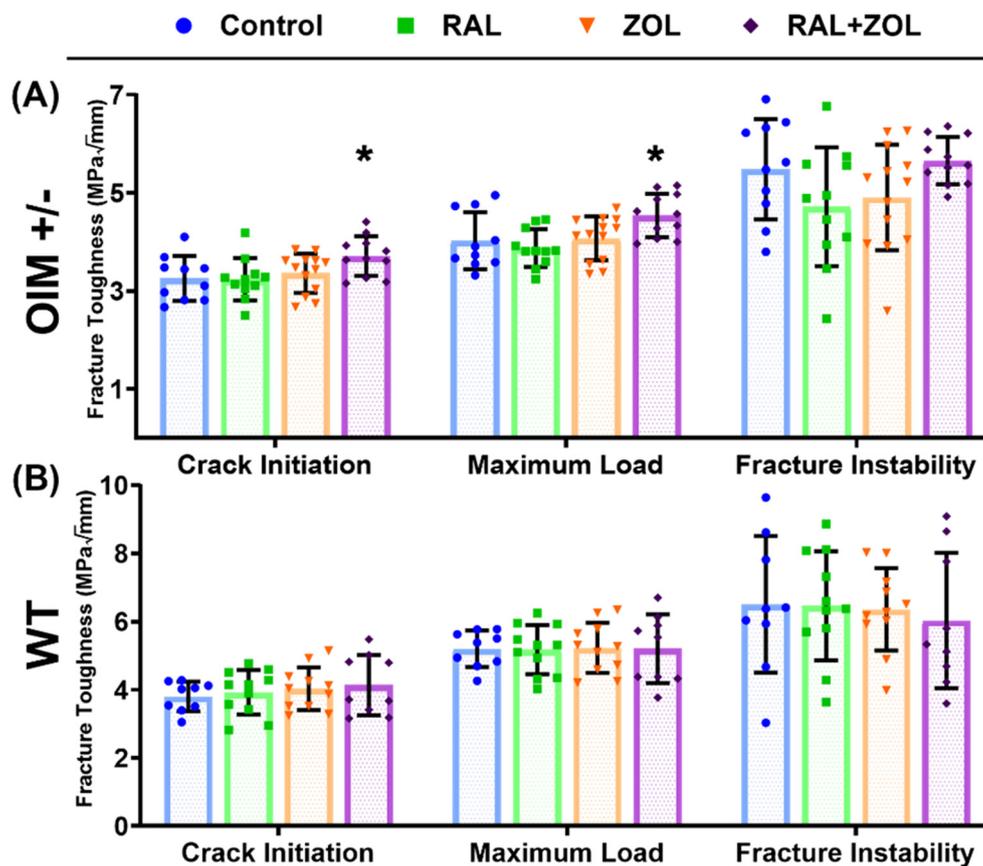

Fig. 3. Treatment effects on the stress intensity factor for crack initiation, maximum load, and fracture instability for OIM +/− (A) and WT (B). Significant change from control indicated by '*' at $p < 0.05$.

been shown to improve with BP treatment. In skeletally mature rabbits, ZOL injections did not improve fracture toughness in ulnar sections [37]. In humans, long term BP use has additionally been shown to compromise fracture toughness on femoral corticocancellous biopsies [38].

BPs are the only FDA approved drug for pharmaceutical treatment of Osteogenesis Imperfecta. A recent review paper compiled over 15 years of clinical trials investigating BPs use in patients with OI. It was determined that while both oral and IV BPs substantially improved BMD, it was unclear whether BPs consistently improve fracture resistance and decrease fracture risk [39]. Continuous use of BPs in children and teenagers with OI has revealed some negative impacts on bone health, including microdamage accumulation and delayed healing [40–42]. These findings confirm the need for treatments that focus on improving bone quality, in addition to quantity, to improve skeletal

fragility and prevent fracture. The fact that we have shown a positive combined treatment effect on measures of fracture resistance in diseased bone, effectively returning these properties to near WT control levels, is promising and future work will focus on treatment strategies to optimize this effect.

There are some limitations to our study. Male mice were chosen in attempt to reduce the metabolic effects of RAL and utilize its cell-independent mechanism. This was intentional but could limit the findings. The study also did not directly compare the effects of treatment on bone cell activity or on extracellular matrix quality. Future work should be conducted to assess treatment effects on both sexes along with further investigation of cellular and matrix activity in the diseased condition. With fracture toughness testing, sample sizes were not consistent across groups. Numerous bones were accidentally broken during the notching process. It was also difficult to determine the transition lines

of crack propagation for several samples. Homozygous (OIM $-/-$) mice were originally included in this study. However, the severity of the phenotype caused numerous spontaneous fractures in the untreated mice, and only 2 control samples were usable for analysis. Lastly, the age of the mice used here could be controversial. The mice received treatment from 8 weeks to 16 weeks. The age group was chosen to mirror the rapid growth during human adolescence, and potentially when treatment might be started in humans with OI. This age could have led to the high deformation in the control groups due to rapid modeling and slow mineralization. It is also problematic because it does not coincide with an age that humans receive RAL, as RAL is typically only administered in older adults. Future studies will also investigate the effects of combined treatment in older animals, following skeletal maturity.

The use of RAL has some limitations in itself. Although RAL possesses beneficial intrinsic effects, it may not necessarily be the most ideal drug to pursue for combinatorial therapy. RAL suppresses bone loss as a selective estrogen receptor modulator (SERM), but this estrogen therapy produces adverse effects such as hot flashes and increased thrombosis risk, making it a problematic treatment. The estrogen receptor binding also prevents usage in some at-risk patient populations including children, specifically those with OI [43,44]. Other drugs could be considered for a combination treatment. Recent work has shown positive outcomes in OI patients and OI mice treated with sclerostin antibody and denosumab [34,45,46]. A more appropriate therapeutic for combination treatment might be parathyroid hormone (PTH) as its anabolic mechanism has been shown to create better quality new bone [47]. Combination of PTH and alendronate has previously been studied clinically for osteoporosis treatment, but results did not indicate any remarkable benefit compared to either monotherapy [48–50]. In OI patients, PTH has been shown to positively impact BMD, but comparison to BP use or a combination treatment was not studied [51]. These compounds, amongst others, should be investigated deeper to determine an ideal combination, concentration, and dosing schedule. Ideally, there is a need to develop pharmaceuticals that, like RAL, directly target collagen and the extracellular matrix to improve quality at the microscopic level, without acting as a SERM [14].

In conclusion, the current study shows beneficial effects of combination therapy, enhancing quality of diseased bone neither treatment could accomplish alone. Utilizing the mass-based effects of ZOL with the tissue material changes of RAL, combined therapy improved fracture toughness and led to increases in trabecular architecture and cortical mechanics in diseased animals. Combinatorial treatments should be considered for future therapies to optimize patient care and bone health.

Declaration of Competing Interest

There are no known conflicts of interest associated with this publication, and there has been no financial support for this work that could have influenced its outcome.

Acknowledgements

Appendix A. Supplementary data

Supplementary data to this article can be found online at https://doi.org/10.1016/j.bone.2019.06.018.

References

[1] R.G. Russell, Bisphosphonates: the first 40 years, Bone 49 (2011) 2–19 Jul.

[2] NIH, Osteoporosis prevention, diagnosis, and therapy, JAMA 285 (2001) 785–795 Feb 14.

[3] F.H. Glorieux, N.J. Bishop, H. Plotkin, G. Chabot, G. Lanoue, R. Travers, Cyclic administration of pamidronate in children with severe osteogenesis imperfecta, N. Engl. J. Med. 339 (Oct 1 1998) 947–952.

[4] R.G. Russell, N.B. Watts, F.H. Ebetino, M.J. Rogers, Mechanisms of action of bisphosphonates: similarities and differences and their potential influence on clinical efficacy, Osteoporos. Int. 19 (2008) 733–759 Jun.

[5] M.R. Allen, D.B. Burr, Bisphosphonate effects on bone turnover, microdamage, and mechanical properties: what we think we know and what we know that we don't know, Bone 49 (2011) 56–65 Jul.

[6] S.Y. Tang, M.R. Allen, R. Phipps, D.B. Burr, D. Vashishth, Changes in non-enzymatic glycation and its association with altered mechanical properties following 1-year treatment with risedronate or alendronate, Osteoporos. Int. 20 (2009) 887–894 Jun.

[7] M.R. Allen, E. Gineyts, D.J. Leeming, D.B. Burr, P.D. Delmas, Bisphosphonates alter trabecular bone collagen cross-linking and isomerization in beagle dog vertebra, Osteoporos. Int. 19 (2008) 329–337 Mar.

[8] C. Acevedo, H. Bale, B. Gludovatz, A. Wat, S.Y. Tang, M. Wang, et al., Alendronate treatment alters bone tissues at multiple structural levels in healthy canine cortical bone, Bone 81 (2015) 352–363 Dec.

[9] H.U. Bryant, Mechanism of action and preclinical profile of raloxifene, a selective estrogen receptor modulation, Rev. Endocr. Metab. Disord. 2 (2001) 129–138 Jan.

[10] E. Seeman, G.G. Crans, A. Diez-Perez, K.V. Pinette, P.D. Delmas, Anti-vertebral fracture efficacy of raloxifene: a meta-analysis, Osteoporos. Int. 17 (2006) 313–316 Feb.

[11] R.R. Recker, B.H. Mitlak, X. Ni, J.H. Krege, Long-term raloxifene for post-menopausal osteoporosis, Curr. Med. Res. Opin. 27 (2011) 1755–1761 Sep.

[12] B. Ettinger, D.M. Black, B.H. Mitlak, R.K. Knickerbocker, T. Nickelsen, H.K. Genant, et al., Reduction of vertebral fracture risk in postmenopausal women with osteoporosis treated with raloxifene: results from a 3-year randomized clinical trial. Multiple Outcomes of Raloxifene Evaluation (MORE) investigators, JAMA 282 (1999) 637–645.

[13] M.A. Gallant, D.M. Brown, M. Hammond, J.M. Wallace, J. Du, A.C. Deymier-Black, et al., Bone cell-independent benefits of raloxifene on the skeleton: a novel mechanism for improving bone material properties, Bone 61 (2014) 191–200. Apr.

[14] N. Bivi, H. Hu, B. Chavali, M.J. Chalmers, C.T. Reutter, G.L. Durst, et al., Structural features underlying raloxifene's biophysical interaction with bone matrix, Bioorg. Med. Chem. 24 (2016) 759–767 Feb 15.

[15] H. Kuivaniemi, G. Tromp, D.J. Prockop, Mutations in fibrillar collagens (types I, II, III, and XI), fibril-associated collagen (type IX), and network-forming collagen (type X) cause a spectrum of diseases of bone, cartilage, and blood vessels, Hum. Mutat. 9 (1997) 300–315.

[16] T. Pihlajaniemi, L.A. Dickson, F.M. Pope, V.R. Korhonen, A. Nicholls, D.J. Prockop, et al., Osteogenesis imperfecta: cloning of a pro-alpha 2(I) collagen gene with a frameshift mutation, J. Biol. Chem. 259 (1984) 12941–12944.

[17] D. W. Rowe and J. R. Shapiro, "Osteogenesis Imperfecta," in *Metabolic Bone Disease and Clinically Related Disorders*, 3 ed: Academic Press, 1998, pp. 651–683.

[18] N. Nicolaou, Y. Agrawal, M. Padman, J.A. Fernandes, M.J. Bell, Changing pattern of femoral fractures in osteogenesis imperfecta with prolonged use of bisphosphonates, J. Child. Orthop. 6 (2012) 21–27 Mar.

[19] J.M. Fritz, Y. Guan, M. Wang, P.A. Smith, G.F. Harris, A fracture risk assessment model of the femur in children with osteogenesis imperfecta (OI) during gait, Med. Eng. Phys. 31 (2009) 1043–1048 2009/11/01/.

[20] O. Johnell, W.H. Scheele, Y. Lu, J.Y. Reginster, A.G. Need, E. Seeman, Additive effects of raloxifene and alendronate on bone density and biochemical markers of bone remodeling in postmenopausal women with osteoporosis, J. Clin. Endocrinol. Metab. 87 (2002) 985–992 Mar.

[21] A. Carriero, E.A. Zimmermann, A. Paluszny, S.Y. Tang, H. Bale, B. Busse, et al., How tough is brittle bone? Investigating osteogenesis imperfecta in mouse bone, J. Bone Miner. Res. 29 (2014) 1392–1401 Jun.

[22] S.M. Carleton, D.J. McBride, W.L. Carson, C.E. Huntington, K.L. Twenter, K.M. Rolwes, et al., Role of genetic background in determining phenotypic severity throughout postnatal development and at peak bone mass in Col1a2 deficient mice (oim), Bone 42 (2008) 681–694.

[23] M.R. Allen, H.A. Hogan, W.A. Hobbs, A.S. Koivuniemi, M.C. Koivuniemi, D.B. Burr, Raloxifene enhances material-level mechanical properties of femoral cortical and trabecular bone, Endocrinology 148 (2007) 3908–3913. Aug.

[24] M.R. Allen, P.R. Territo, C. Lin, S. Persohn, L. Jiang, A.A. Riley, et al., In vivo UTE-MRI reveals positive effects of raloxifene on skeletal-bound water in skeletally mature dogs, J. Bone Miner. Res. 30 (2015) 1441–1444. Aug.

[25] M.W. Aref, E.M. McNerny, D. Brown, K.J. Jepsen, M.R. Allen, Zoledronate treatment has different effects in mouse strains with contrasting baseline bone mechanical phenotypes, Osteoporos. Int. 27 (2016) 3637–3643 Dec.

[26] A.G. Berman, J.M. Wallace, Z.R. Bart, M.R. Allen, Raloxifene reduces skeletal fractures in an animal model of osteogenesis imperfecta, Matrix Biol. 52-54 (2016) 19–28 May-Jul.

[27] A.G. Berman, C.A. Clauser, C. Wunderlin, M.A. Hammond, J.M. Wallace, Structural and mechanical improvements to bone are strain dependent with axial compression of the tibia in female C57BL/6 mice, PLoS One 10 (2015) e0130504.

[28] J.M. Wallace, K. Golcuk, M.D. Morris, D.H. Kohn, Inbred strain-specific response to biglycan deficiency in the cortical bone of C57BL6/129 and C3H/He mice, J. Bone Miner. Res. 24 (2009) 1002–1012 Jun.

[29] M.A. Hammond, A.G. Berman, R. Pacheco-Costa, H.M. Davis, L.I. Plotkin, J.M. Wallace, Removing or truncating connexin 43 in murine osteocytes alters cortical geometry, nanoscale morphology, and tissue mechanics in the tibia, Bone 88 (2016) 85–91 Jul.

[30] R.O. Ritchie, K.J. Koester, S. Ionova, W. Yao, N.E. Lane, J.W. Ager 3rd, Measurement of the toughness of bone: a tutorial with special reference to small animal studies, Bone 43 (2008) 798–812 Nov.

[31] R. Bargman, R. Posham, A.L. Boskey, E. DiCarlo, C. Raggio, N. Pleshko, Comparable outcomes in fracture reduction and bone properties with RANKL inhibition and alendronate treatment in a mouse model of osteogenesis imperfecta, Osteoporos. Int. 23 (2012) 1141–1150 Mar.

[32] C.N. Meixner, M.W. Aref, A. Gupta, E.M.B. McNerny, D. Brown, J.M. Wallace, et al., Raloxifene improves bone mechanical properties in mice previously treated with zoledronate, Calcif. Tissue Int. 101 (2017) 75–81 Jul.

[33] B.M. Misof, P. Roschger, T. Baldini, C.L. Raggio, V. Zraick, L. Root, et al., Differential effects of alendronate treatment on bone from growing osteogenesis imperfecta and wild-type mouse, Bone 36 (2005) 150–158 Jan.

[34] D. Olvera, R. Stolzenfeld, J.C. Marini, M.S. Caird, K.M. Kozloff, Low dose of bi-sphosphonate enhances sclerostin antibody-induced trabecular bone mass gains in Brtl/+ osteogenesis imperfecta mouse model, J. Bone Miner. Res. 33 (2018) 1272–1282 Jul.

[35] L. Imbert, J.-C. Aurégan, K. Pernelle, T. Hoc, Microstructure and compressive me-chanical properties of cortical bone in children with osteogenesis imperfecta treated with bisphosphonates compared with healthy children, J. Mech. Behav. Biomed. Mater. 46 (2015) 261–270 (2015/06/01/).

[36] V. Vardakastani, D. Saletti, W. Skalli, P. Marry, J.M. Allain, C. Adam, Increased intra-cortical porosity reduces bone stiffness and strength in pediatric patients with osteogenesis imperfecta, Bone 69 (2014) 61–67 Dec.

[37] M.D. Hunckler, E.D. Chu, A.P. Baumann, T.E. Curtis, M.J. Ravosa, M.R. Allen, et al., The fracture toughness of small animal cortical bone measured using arc-shaped tension specimens: effects of bisphosphonate and deproteinization treatments, Bone 105 (2017) 67–74 Dec.

[38] A.A. Lloyd, B. Gludovatz, C. Riedel, E.A. Luengo, R. Saiyed, E. Marty, et al., Atypical fracture with long-term bisphosphonate therapy is associated with altered cortical composition and reduced fracture resistance, Proc. Natl. Acad. Sci. U. S. A. 114 (2017) 8722–8727. Aug 15.

[39] K. Dwan, C.A. Phillipi, R.D. Steiner, D. Basel, Bisphosphonate therapy for osteogenesis imperfecta (in eng), Cochrane Database Syst. Rev. 7 (2014) p. Cd005088.

[40] E.A. Anam, F. Rauch, F.H. Glorieux, F. Fassier, R. Hamdy, Osteotomy healing in children with osteogenesis imperfecta receiving bisphosphonate treatment, J. Bone Miner. Res. 30 (2015) 1362–1368. Aug.

[41] S.E. Papapoulos, S.C. Cremers, Prolonged bisphosphonate release after treatment in children, N. Engl. J. Med. 356 (2007) 1075–1076 Mar 8.

[42] R.F. Vasanwala, A. Sanghrajka, N.J. Bishop, W. Hogler, Recurrent proximal femur fractures in a teenager with osteogenesis imperfecta on continuous bisphosphonate therapy: are we overtreating? J. Bone Miner. Res. 31 (2016) 1449–1454 Jul.

[43] A. Qaseem, M.A. Forciea, R.M. McLean, T.D. Denberg, Treatment of low bone density or osteoporosis to prevent fractures in men and women: a clinical practice guideline update from the American College of Physicians, Ann. Intern. Med. 166 (2017) 818–839 Jun 6.

[44] I.R. Reid, Efficacy, effectiveness and side effects of medications used to prevent fractures, J. Intern. Med. 277 (2015) 690–706 Jun.

[45] F.H. Glorieux, J.P. Devogelaer, M. Durigova, S. Goemaere, S. Hemsley, F. Jakob, et al., BPS804 anti-sclerostin antibody in adults with moderate osteogenesis im-perfecta: results of a randomized phase 2a trial, J. Bone Miner. Res. 32 (2017) 1496–1504 Jul.

[46] H. Hoyer-Kuhn, J. Franklin, G. Allo, M. Kron, C. Netzer, P. Eysel, et al., Safety and efficacy of denosumab in children with osteogenesis imperfect–a first prospective trial, J. Musculoskelet. Neuronal Interact. 16 (2016) 24–32 Mar.

[47] M. Sato, G.Q. Zeng, C.H. Turner, Biosynthetic human parathyroid hormone (1–34) effects on bone quality in aged ovariectomized rats, Endocrinology 138 (1997) 4330–4337.

[48] D.M. Black, S.L. Greenspan, K.E. Ensrud, L. Palermo, J.A. McGowan, T.F. Lang, et al., The Effects of Parathyroid Hormone and Alendronate Alone or in Combination in Postmenopausal Osteoporosis, vol. 349, (2003), pp. 1207–1215.

[49] J.S. Finkelstein, A. Hayes, J.L. Hunzelman, J.J. Wyland, H. Lee, R.M. Neer, The Effects of Parathyroid Hormone, Alendronate, or Both in Men with Osteoporosis, vol. 349, (2003), pp. 1216–1226.

[50] S. Khosla, Parathyroid Hormone plus Alendronate — A Combination That Does Not Add up, vol. 349, (2003), pp. 1277–1279.

[51] E.S. Orwoll, J. Shapiro, S. Veith, Y. Wang, J. Lapidus, C. Vanek, et al., Evaluation of teriparatide treatment in adults with osteogenesis imperfecta, J. Clin. Invest. 124 (2014) 491–498 02/03/.